

# Magnetic thaw down and boil-off of electrons in the quantum Hall effect regime due to magnetoacceptors in GaAs/GaAlAs heterostructures

I. Bisotto,<sup>1</sup> C. Chaubet,<sup>2,\*</sup> A. Raymond,<sup>2</sup> J. C. Harmand,<sup>3</sup> M. Kubisa,<sup>4</sup> and W. Zawadzki<sup>5</sup>

<sup>1</sup>LNCMI, UPR 3228, CNRS-INSA-UJF-UPS, BP166, 38042 Grenoble, Cedex 9, France

<sup>2</sup>L2C UMR 5221, CNRS-Université Montpellier 2, Place E. Bataillon, 34090 Montpellier cedex 05, France

<sup>3</sup>LPN, CNRS, route de Nozay, 91460 Marcoussis, France

<sup>4</sup>Institute of Physics, Wrocław University of Technology, 50-370 Wrocław, Poland

<sup>5</sup>Institute of Physics, Polish Academy of Sciences, 02668 Warsaw, Poland

(Received 16 April 2012; published 27 August 2012)

The quantum Hall effect (QHE) and the Shubnikov–de Haas effect in the QHE regime are investigated experimentally using modulation doped *n*-type GaAs/GaAlAs quantum wells additionally doped in the well with beryllium. It is known that acceptor states introduced by Be atoms have a localized character in the conduction band due to a combined effect of the well and a magnetic field parallel to the growth direction and that they possess discrete energies above the corresponding conduction Landau levels. It is presently shown that the localized magnetoacceptor (MA) states lead to two observable effects in magnetotransport in the ultraquantum limit: magnetic thaw down and magnetic boil-off of two-dimensional (2D) electrons. Both effects are related to the fact that electrons occupying localized MA states cannot conduct. Thus in the thaw down effect the electrons fall down from the MA states to the free Landau states, which leads to a shift of the Hall plateau toward higher magnetic fields as a consequence of an increase of the 2D electron density  $N_s$ . In the boil-off effect the electrons are pushed from the free Landau states to the MA states which leads to a dramatic increase of resistance, as a consequence of the decrease of  $N_s$ . Differences between the above effects and those induced by magnetodonors in 2D systems are emphasized. We analyze the magnetic boil-off effect theoretically assuming that it is caused by the quantum Hall electric field present in our experiments. It is demonstrated that a sufficiently strong electric field in the crossed-field configuration can indeed populate localized MA states above the Landau levels.

DOI: [10.1103/PhysRevB.86.085321](https://doi.org/10.1103/PhysRevB.86.085321)

PACS number(s): 73.20.Jc, 73.20.Hb, 73.43.Cd

## I. INTRODUCTION

Impurities play an important role in the physical phenomena observed on a two-dimensional electron gas (2DEG) confined in semiconductor heterostructures. Impurities provide one of the dominant scattering modes for electrons, they are also a source of 2D electrons in quantum wells (QW). Using the possibilities of modulation doping the impurities can be introduced directly into the well as well as into confining barriers. In a large majority of cases donors are introduced into the barriers in order to provide electrons without reducing their mobility. The presence of donors results in smooth long-range potential fluctuations, both attractive and repulsive. In consequence, in the presence of a magnetic field the Landau levels (LLs) are almost symmetrically broadened,<sup>1–3</sup> giving rise to the well known quantum Hall effect.<sup>4,5</sup>

Some time ago new discrete states in the conduction bands of heterostructures were proposed by Kubisa and Zawadzki.<sup>6</sup> These states are introduced into the conduction band by magnetoacceptors placed in the well. Usually an acceptor, being a negatively charged center, repulses a conduction electron. However, in a QW a combined effect of the confining potential and of the Lorentz force caused by magnetic field parallel to the growth direction keeps the electron near the acceptor. In our QWs the additional acceptor potentials are not random. The acceptors are put by selective doping into specific planes of the GaAs well or at the GaAlAs/GaAs interface. Thus the repulsive potentials are strong and they have short-range character. They result in discrete electron levels above free electron LLs. The existence of such states in GaAs/GaAlAs heterostructures was convincingly demon-

strated with the use of interband and intraband magneto-optical experiments.<sup>7,8</sup>

The purpose of the present paper is to demonstrate the effect of discrete states due to magnetoacceptors in magnetotransport phenomena. The role of impurities in magnetotransport experiments is particularly important. For example, the width of the quantum Hall plateaus depends strongly on the impurity concentration.<sup>9</sup> Haug *et al.*<sup>10</sup> showed that the nature of impurities, attractive or repulsive, introduces an asymmetry of the Hall plateaus with respect to the classical Hall effect:  $\rho_{xy}^o = B/N_s e$ . For donor-doped samples the plateaus shift toward lower magnetic fields (i.e., larger filling factors  $\nu = hN_s/eB$ ), whereas for acceptor-doped samples the plateaus shift toward higher magnetic fields (smaller filling factors). The results were interpreted in terms of an asymmetry of the density of states. In another study, performed on Si metal-oxide-semiconductor field-effect transistors, Furneaux and Reinecke<sup>11</sup> investigated the effect of driftable Na<sup>+</sup> ions on the width and position of Hall plateaus. Also these authors interpreted their results in terms of an asymmetric distribution of localized states on the edges of overlapping Landau levels. Raymond *et al.*<sup>12</sup> studied experimentally and theoretically the effects of additional attractive or repulsive ionized impurities on the resistivity components  $\rho_{xx}$  and  $\rho_{xy}$  in the QHE regime. The authors investigated experimentally a number of GaAs/GaAlAs asymmetric modulation-doped QWs with additional  $\delta$  doping by Si donors or Be acceptors in the GaAs channel or at the AlGaAs/GaAs interface. The main result of this study is that the whole  $\nu = 1$  plateau of QHE shifts with respect to the classical Hall effect in case of additional

doping with acceptors. In the present paper we will show that the shift of the  $\nu = 1$  Hall plateau can be explained by the existence of localized magnetoacceptor states above the free Landau states. We call the electron transfer from the upper localized states to the lower Landau states, as a magnetic field increases, the thaw down effect. We will also show that, in the ultraquantum limit of magnetic fields, the Hall electric field can push the conducting electrons from the free Landau states to the localized acceptor states at higher energies. This process, which we call the boil-off effect, can be considered to be an inverse process to the freeze-out effect in which the conducting electrons from the free Landau states fall to localized donor states at lower energies.<sup>13</sup>

Our paper is organized as follows. In Sec. II we present characteristics of the investigated samples as well as experimental techniques. Section III describes an experimental study of the magnetic thaw down of 2D electrons from magnetoacceptor states in the ultraquantum limit, as well as an experimental study of the electron boil-off effect into magnetoacceptor states. Section IV contains a theory in which we calculate probabilities of electron transitions from the Landau states to magnetoacceptor states due to ionized impurities and acoustic phonons in the presence of a strong electric field in the crossed-field configuration. In Sec. V we briefly discuss our results, the paper is concluded by a summary.

## II. SAMPLE CHARACTERISTICS AND EXPERIMENTAL TECHNIQUES

Our samples were modulation-doped GaAs/Ga<sub>1-x</sub>Al<sub>x</sub>As asymmetric single quantum wells grown by molecular beam epitaxy. As shown in Fig. 1, all investigated samples were  $\delta$  doped in the GaAlAs barrier on one side, forming two planes of Si donors: The one closer to the interface contained parent donors providing the conducting 2D electrons. Moreover, except for the reference samples, additional Be impurities were introduced via a  $\delta$ -doped layer located either at the interface or in the quantum well. The characteristics of the investigated samples are given in Table I.

Two different techniques were used in transport experiments performed on symmetric double-cross samples. In the first technique we impose the current and measure voltage drop across the sample. This is done with a dc current

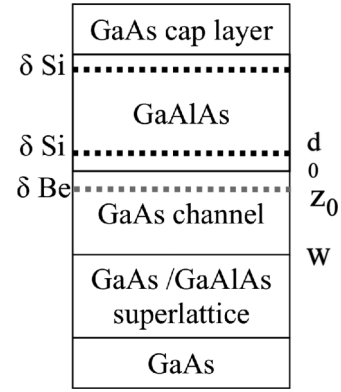


FIG. 1. Typical structure of modulation doped GaAs/GaAlAs quantum wells:  $z_0$  is the position of the  $\delta$  layer of additional acceptors,  $d$  is the spacer thickness, and  $w$  is the width of the GaAs channel.

source Keithley 220 and HP 34401 voltmeters to measure the Hall voltage ( $V_{xy}$ ) and the Shubnikov–de Haas voltage ( $V_{xx}$ ) within a current intensity range 10 nA–10  $\mu$ A. In the second technique we impose the voltage and measure the current. This is performed using an ac voltage generator of EGG lock-in amplifiers 7225, as well as a current amplifier NF LI 76. A low-frequency voltage (17 Hz) was applied to the sample, current and voltages were measured at the same frequency.

## III. EXPERIMENTAL STUDY OF MAGNETIC THAW DOWN AND BOIL-OFF EFFECTS

In this section we describe results obtained using both techniques, that is, using either a current-driven source or a voltage-driven source. We begin with the results obtained with the dc current-driven source. The low current density was equal to 10 or 100 nA (see Figs. 2 to 5). Next we present results obtained at higher currents (up to a few  $\mu$ A) shown in Figs. 7 and 8. Finally, we present results obtained using a voltage-driven ac source, see Figs. 9 and 10.

We observed that, at low currents, all the reference samples exhibited for the filling factor  $\nu = 1$ , a common crossing point of the Hall plateaus at different temperatures, including the crossing with the classical Hall line (see Fig. 2). The Hall plateaus, as well as the corresponding field regions where

TABLE I. Samples characteristics:  $N_A$  is the density of additional acceptors,  $x$  is the Al percentage,  $N_s$  is the density of 2D electrons,  $\mu$  is the mobility of 2D electrons at low temperatures, and  $\Delta N_s$  is the additional electron density. In sample 35A54 there are two additional Be-doping layers.

Samples	Add. Acceptors $N_A$ (cm <sup>-2</sup> )	$x$ (%)	$z_0$ (Å)	$d$ (Å)	$w$ (Å)	$N_s$ ( $\times 10^{11}$ cm <sup>-2</sup> )	$\mu$ ( $\times 10^5$ cm <sup>2</sup> /V s)	$\Delta N_s$ ( $\times 10^{11}$ cm <sup>-2</sup> )
S908	Reference (0)	25		400	250	2.2	8.9	
B9B11	Reference (0)	33		250	250	2.05	4	
B9B18	Be ( $1 \times 10^{10}$ )	33	+20	250	250	2.18	0.8	$1.3 \times 10^{10}$
35A52	Reference (0)	26.8		400	250	2.7	5	
35A53	Be ( $2 \times 10^{10}$ )	26.8	+25	400	250	2.5	0.88	$2.1 \times 10^{10}$
	( $2 \times 10^{10}$ )		0					
35A54	Be	26.8		400	250	2.25	0.36	$3.8 \times 10^{10}$
	( $2 \times 10^{10}$ )		+25					
35A55	Be ( $4 \times 10^{10}$ )	26.8	+25	400	250	1.36	0.53	$3.5 \times 10^{10}$

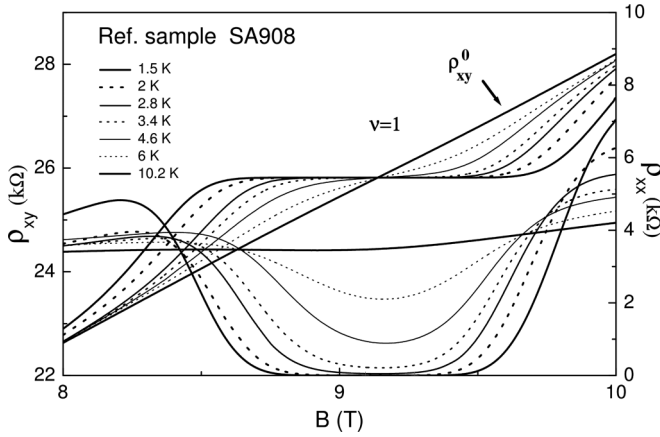


FIG. 2. Transport characteristics at low current around the filling factor  $\nu = 1$  of reference sample SA908 at different temperatures versus magnetic field. The Hall plateau as well as the region of  $\rho_{xx} = 0$  are symmetric with respect to the crossing point of the Hall resistance  $\rho_{xy}^0$ .

$\rho_{xx} = 0$ , were still symmetric with respect to this crossing point. In consequence, this point in the middle of the plateau  $\nu = 1$  can be used to determine 2DEG density  $N_s$ , see Fig. 2.

For structures with additional acceptor impurities we observe a shift toward higher magnetic fields of the  $\nu = 1$  plateau, see Fig. 3. However, under quantizing magnetic field, the crossing point between the higher temperature Hall curves and the lower temperature Hall curves is still in the middle of the  $\nu = 1$  plateau, see Fig. 4. We observe for all the investigated samples with additional acceptor states that, as the temperature is increased, the  $\nu = 1$  plateau disappears and is replaced by an inflexion point, while even- $\nu$  plateaus are still well defined. This shows that, although exchange effects leading to the enhancement of the spin splitting almost disappear at higher temperatures, the Hall line still crosses the low-temperature  $\nu = 1$  Hall plateau in the middle. Thus the crossing point does not depend on the temperature. The shift  $\Delta B$  of the middle of  $\nu = 1$  plateau increases with the

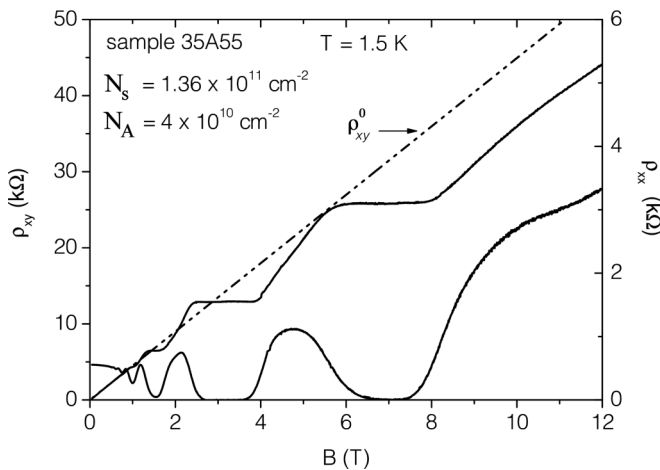


FIG. 3. Transport characteristics at low current of sample 35A55 doped with high density of additional acceptors versus magnetic field. A clear shift of  $\nu = 1$  plateau toward higher magnetic fields with respect to the classical Hall line is observed.

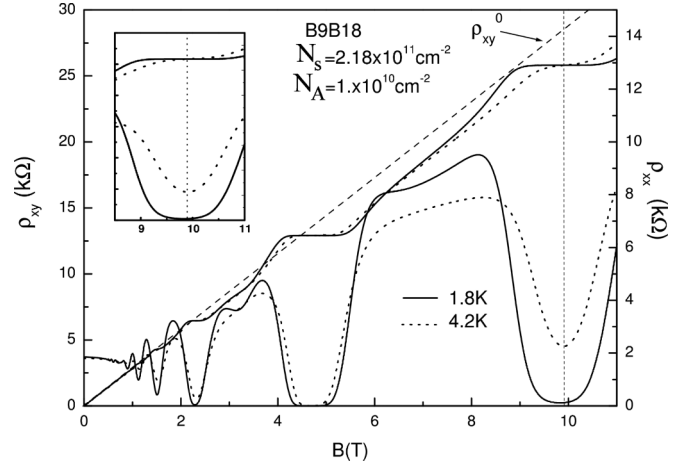


FIG. 4. Transport characteristics at low current of sample B9B18 at  $T = 1.8$  K and  $T = 4.2$  K versus magnetic field. A shift of  $\nu = 1$  plateau is observed but the crossing point between the Hall resistance at both temperatures is still in the middle of the  $\nu = 1$  plateau, as shown in the inset.

density of additional acceptors, see Fig. 5. If we reasonably assume that this point still gives the value of  $N_s$  at the corresponding magnetic field, we measure experimentally an increase  $\Delta N_s$  which is approximately equal to the density  $N_A$  of Be acceptors, see Table I. As shown in Fig. 6, for magnetic fields higher than that corresponding to  $\nu = 2$ , the Fermi level is between the acceptor levels  $0_A^\pm$  and the Landau levels  $0^\pm$ , so that the electrons from the localized states  $0_A^\pm$  fall down to the  $0^\pm$  Landau states and they can conduct. We call this process the thaw down effect. It is manifested by the experimentally verified equality  $N_A \approx \Delta N_s$ , saying that the additional free electron density  $\Delta N_s$  comes from the emptying of acceptor states. This effect is a direct consequence of the particularity of magnetoacceptor states which represent localized states

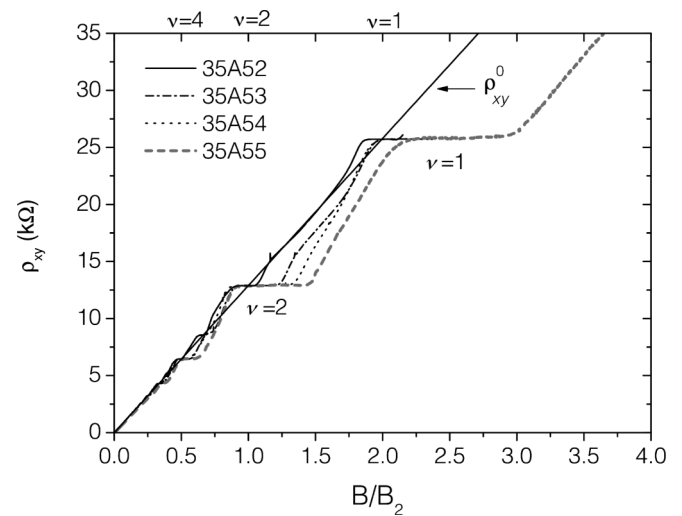


FIG. 5. Hall resistivity at low current, at  $T = 1.5$  K, normalized by the value of  $B_2$ , corresponding to the filling factor  $\nu = 2$ , for four samples with different acceptor densities (see Table I). The shift  $\Delta B$  of the middle of the  $\nu = 1$  plateau increases with the density of additional acceptors, which is a manifestation of the thaw down effect.

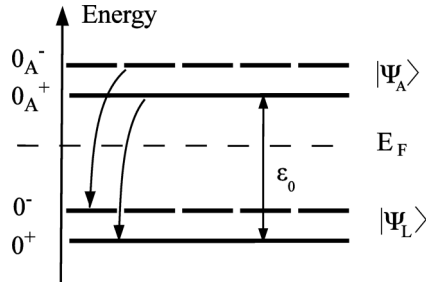


FIG. 6. Free Landau states and discrete magnetoacceptor states in the QHE regime. As the magnetic field is increased and the Fermi level is below acceptors levels, the localized electrons at acceptors thaw down into delocalized Landau states, see text.

above the corresponding free Landau states. We mention that in samples with low densities of additional acceptors and high electron mobilities the thaw down effect was observed also at very low temperatures for the filling factor  $\nu = 3$ .<sup>16</sup>

Next we consider magnetotransport phenomena observed at higher currents. In the plateau region the Hall resistivity  $\rho_{xy}$  is quantized in integer values of  $h/e^2$ , while the longitudinal resistivity  $\rho_{xx}$  vanishes giving rise to a dissipationless state. Ebert *et al.*<sup>14</sup> and Cage *et al.*<sup>15</sup> demonstrated that the dissipationless state suddenly disappears when the electric current exceeds a critical value. This is the so-called QHE breakdown. Many experimental and theoretical studies were carried out to understand the origin of this phenomenon (see Ref. 12 and the references therein). In our current-driven experiments we observed the QHE breakdown when the current density was increased, see Fig. 7. However, for samples with additional acceptors, and particularly for sample 35A55 whose density of Be atoms  $N_A = 4 \times 10^{10} \text{ cm}^{-2}$  is nearly equal to one third of the electron density  $N_s$ , instead of the QHE breakdown a huge increase was observed for both  $\rho_{xx}$  and  $\rho_{xy}$  resistivities at magnetic fields beyond  $\nu = 1$ , see Fig. 8.

In order to verify these surprising results we performed transport experiments using the voltage-driven technique. In this case, instead of applying a dc current, we applied an ac voltage on opposite ends of the sample. For samples without

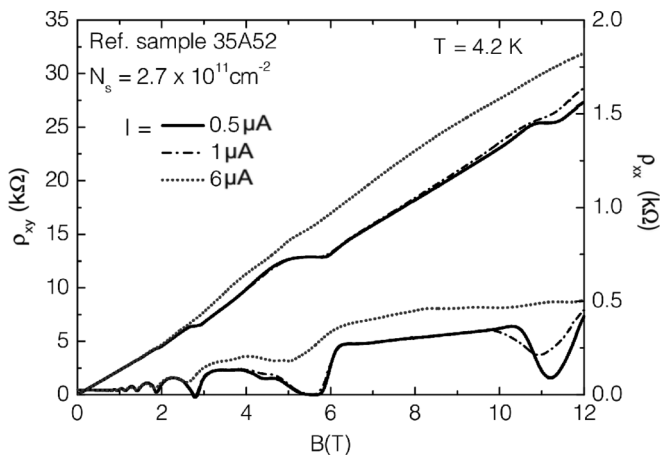


FIG. 7. Transport characteristics of reference sample 32A52 measured for higher currents in dc experiments. Breakdown of QHE is observed at higher currents.

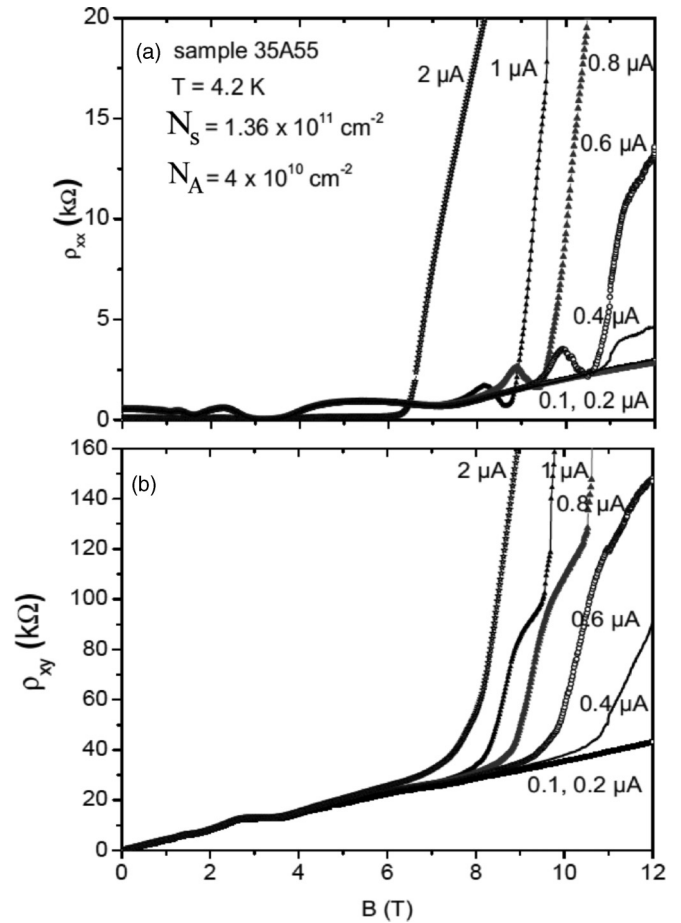


FIG. 8. Transport characteristics of sample 35A55 measured for higher currents in dc experiments. At higher currents a sharp increase of both  $\rho_{xx}$  and  $\rho_{xy}$  is observed in the ultraquantum limit of magnetic field  $\nu < 1$ .

additional acceptors, when the voltage was increased, we observed the well known QHE breakdown, see Fig. 9.

The main effect is an increase of  $\rho_{xx}$ , particularly in the plateau regime. The effect of breakdown on  $\rho_{xy}$  is small, as seen in Fig. 9(b). In contrast, for sample 35A55 we observe a dramatic difference between the low-voltage and high-voltage curves, see Fig. 10. At the field  $B = 12 \text{ T}$  and the polarization voltage 1V the resistance  $\rho_{xy}$  increases up to 140 k $\Omega$ , whereas for the voltage 10 mV it is always below 40 k $\Omega$ . The phenomenon reported in Figs. 8 and 10 on sample 35A55 occurred when the magnetic field was above the value of 6 T corresponding to the filling factor  $\nu = 1$ .

We interpret this large increase of resistivity components as a consequence of a strong decrease of 2DEG density  $N_s$  caused by an increasing Hall electric field  $F_y$ . In our experiments the Hall electric field is always stronger than the applied driving field  $F_x$ . This is particularly true in the ultraquantum limit when the filling factor reaches  $\nu = 1$ . We demonstrate in Sec. IV that a sufficiently high Hall electric field induces transitions of electrons into empty localized acceptor states (the boil-off effect). This effect diminishes the free-carrier density. The existence of empty acceptor states implies that the Fermi level is below them which occurs in the ultraquantum limit. We mention that in the quantum limit, that is, for larger

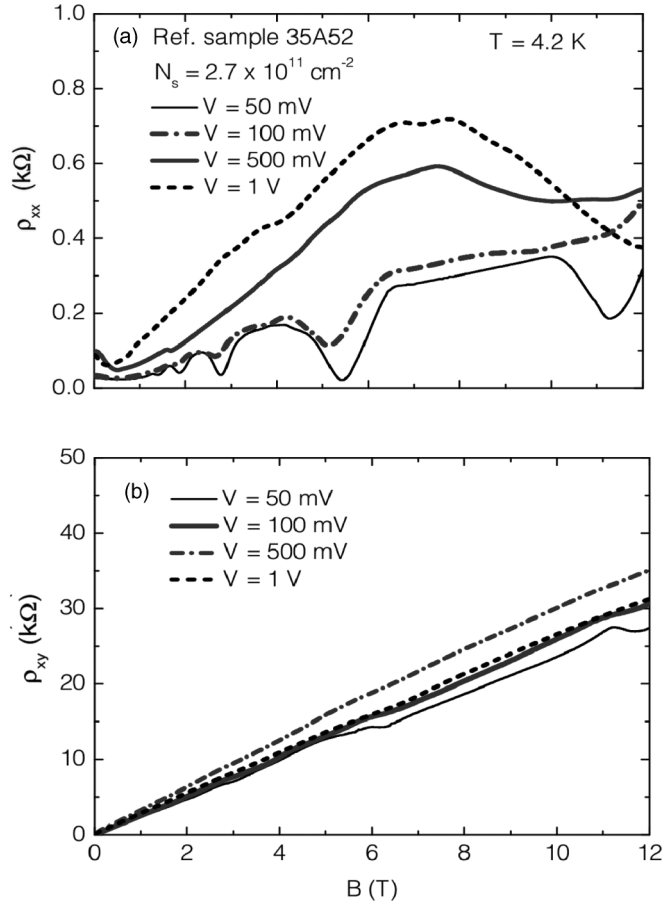


FIG. 9. Transport characteristics of reference sample 32A52 measured for different voltages in ac experiments. At higher voltages the breakdown of QHE is observed.

values of the filling factor ( $\nu = 2, 3, \dots$ ) the situation for boil-off is less favorable: The Hall electric field  $F_y$  is much smaller (two, three times) and the total density  $N_s$  of 2D electrons is distributed on several Landau levels. Consequently the process of localization on empty acceptor states is only efficient for a fraction of 2D electrons ( $1/2, 1/3, \dots$ ).

We observe that the resistivity components measured with the current-driven technique (see Fig. 8) have a steeper slope as functions of the magnetic field than the ones obtained using the voltage-driven measurements (Fig. 10). In our dc conditions the boil-off process has an avalanche character because an increase of  $F_y$  induces a decrease of  $N_s$ , which in turn induces an increase of the Hall voltage when the current is kept constant, and consequently an increase of  $F_y$ . This is what we observe.

#### IV. THEORY

We demonstrate here that, in the presence of a sufficiently high Hall electric field, electrons can make transitions between free Landau states  $|\psi_L\rangle$  and magneto-acceptor states  $|\psi_A\rangle$ . The transitions are induced by the impurity scattering or by the acoustical phonon scattering. They result in a new statistical occupation of the localized acceptor states and a new value of the number of conducting electrons.

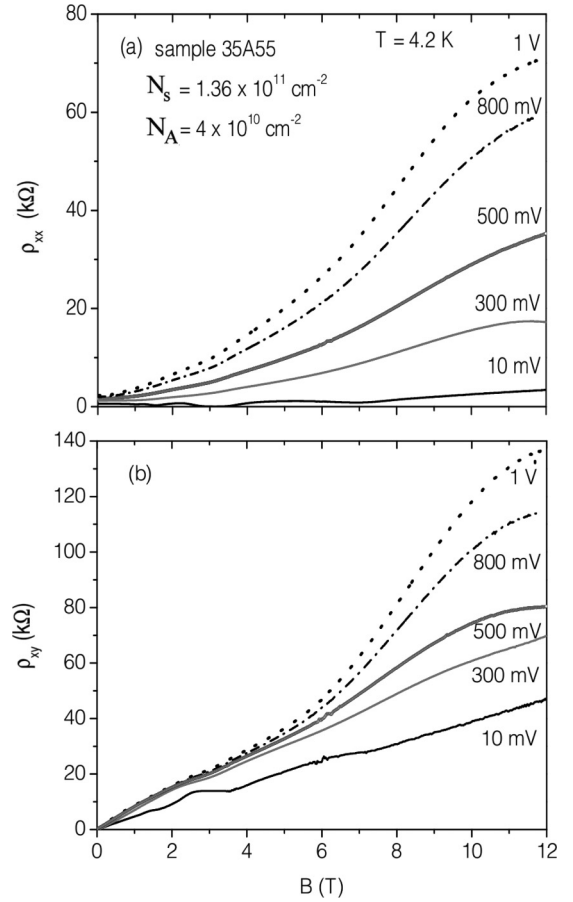


FIG. 10. Transport characteristics of sample 35A55 measured for different voltages in ac experiments. At higher voltages a strong increase of the Hall and longitudinal resistivities are observed.

We demonstrate first that, in the presence of a sufficiently high Hall electric field, electrons can make transitions from free Landau states  $|\psi_L\rangle$  into magnetoacceptor states  $|\psi_A\rangle$ . In the QHE regime, the electron is subjected to an external magnetic field  $\mathbf{B}$  and the Hall electric field  $\mathbf{F}$  in the perpendicular direction. Thus we deal with the electron in crossed electric and magnetic fields, and the current flows in the direction perpendicular to both  $\mathbf{B}$  and  $\mathbf{F}$ . The quantum eigenenergies for this problem are

$$E = \left(n + \frac{1}{2}\right) \hbar \omega_c - eFY_0 - \frac{1}{2} m^* \frac{F^2}{B^2}, \quad (1)$$

where  $\omega_c = eB/m^*$  and  $Y_0 = k_x l_B^2$  is the center of the magnetic motion if we choose the asymmetric gauge  $\mathbf{A} = [-By, 0, 0]$ . In the following we consider the Landau level  $n = 0$  and omit the shift of all levels due to the electric field given by the last term in Eq. (1). As indicated above, localized magnetoacceptor states have energies above the free Landau states.<sup>6</sup> For an acceptor centered at  $\mathbf{r}_0(x_0, y_0)$  a variational wave function  $|\psi'_A\rangle$  is

$$\langle \mathbf{r} | \psi'_A \rangle = \psi'_A(\mathbf{r} - \mathbf{r}_0) = C e^{-\frac{\alpha^2}{4} |\mathbf{r} - \mathbf{r}_0|^2 - \beta |\mathbf{r} - \mathbf{r}_0|}, \quad (2)$$

where  $\alpha$  and  $\beta$  are the variational parameters and  $l_B = \sqrt{\hbar/eB}$  is the magnetic length.<sup>6</sup> The above wave function is characterized by the the quantum numbers  $N = 0$  and  $M = 0$ ,

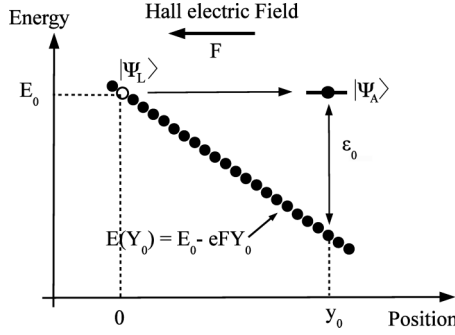


FIG. 11. A free 2D electron makes a transition to a magnetoacceptor state. The displacement  $y_0$  is defined by the distance for which the electrostatic potential loss is compensated by the positive acceptor energy  $\epsilon_0$ .

where  $M$  is the eigenvalue of the angular momentum. We remark that this function is written for the symmetric gauge  $\mathbf{A} = [-By/2, Bx/2, 0]$ . The binding energy of this state is  $\epsilon_0 = 1.85$  meV at  $B = 5$  T (see Ref. 6 for the calculation of the binding energy in the GaAs/GaAlAs quantum well). The corresponding variational parameters are  $\alpha = 0.9/a_0$  and  $\beta = 0.2/a_0$ , where  $a_0$  is the effective Bohr radius for GaAs:  $a_0 = 94$  Å. In the presence of the Hall electric field, a localized acceptor state can have the same energy as a free Landau state, see Fig. 11. Therefore, as a consequence of impurity interactions, a 2D electron can make a transition from the free state centered at the origin to the localized state centered at  $\mathbf{r}_0$ . This is related to a displacement of the orbit center  $y_0$ .

Our calculation of the transition rate for one electron is based on the Fermi golden rule for the impurity-induced transitions between the free state  $|\psi_L\rangle$  whose energy is  $E_0$ , and the acceptor state  $|\psi_A\rangle$  whose energy is  $E_A = E_0 - eFy_0 + \epsilon_0$ , where we have put  $Y_0 = y_0$ , see Fig. 11. We start with the general expression for impurity-induced transitions in two dimensions (see Ref. 16),

$$W_{\mathbf{r}_0} = \frac{2\pi}{\hbar} \delta(E_A - E_0) \left| \int_r d^3r |f_0(z)|^2 \psi_L(\mathbf{r}) \psi_A(\mathbf{r} - \mathbf{r}_0) V(r) \right|^2, \quad (3)$$

where  $V(r)$  is the impurity Coulomb potential and  $f_0(z)$  is the envelope function of the first electric subband. We describe the ground Landau state for  $n = 0$  in the form

$$\langle \mathbf{r} | \psi'_L \rangle = \psi'_L(\mathbf{r}) = \frac{1}{\sqrt{2\pi} l_B} e^{-r^2/4l_B^2}. \quad (4)$$

Also this function is written in the symmetric gauge and is characterized by the quantum numbers  $N = 0$  and  $M = 0$ . When performing the calculations below we transform both functions  $\langle \mathbf{r} | \psi'_A \rangle \rightarrow \langle \mathbf{r} | \psi_A \rangle$  and  $\langle \mathbf{r} | \psi'_L \rangle \rightarrow \langle \mathbf{r} | \psi_L \rangle$  into the asymmetric gauge in order to be consistent with the gauge used in Eq. (1), see the Appendix. Using Eqs. (2) and (4) we neglect the effect of the electric field on  $\psi'_A(\mathbf{r})$  and  $\psi'_L(\mathbf{r})$  wave functions.

Equation (3) takes into account an effective 2D potential averaged over the envelope function  $f_0(z)$ . With the help of

Ref. 1 this integral can be written in the form

$$W_{r_0} = \frac{2\pi}{\hbar} \delta(E_A - E_0) \left| \int_{\mathbf{q}_\perp} d^2q_\perp \frac{S}{(2\pi)^2} f_{A,L}^{2D}(\mathbf{q}) F_i(q_\perp) \right|^2, \quad (5)$$

where  $f_{A,L}^{2D}(\mathbf{q})$  is the form factor of the 2D wave function,

$$f_{A,L}^{2D}(\mathbf{q}) = \int_{x,y} \psi_L(\mathbf{r}) \psi_A(\mathbf{r} - \mathbf{r}_0) e^{i\mathbf{q}_\perp \cdot \mathbf{r}} dx dy, \quad (6)$$

whereas the envelope function  $f_0(z)$  is included in  $F_i$ ,<sup>1</sup>

$$F_i(q_\perp, z_i) = \frac{e^2}{2S\kappa(q_\perp + q_s)} \int_{-\infty}^{\infty} |f_0(z)|^2 e^{-q_\perp |z - z_i|} dz. \quad (7)$$

Here  $\kappa$  is the dielectric permittivity of GaAs (we take  $\kappa = 12.8$  following Ref. 6). If we assume that the impurity is located in the well at the maximum of  $f_0(z)$ , there is  $z_i = 0$  and Eq. (7) becomes

$$F_i(q_\perp, z_i) = \frac{e^2}{2S\kappa(q_\perp + q_s)} \frac{1}{(1 + q_\perp/b)^3}. \quad (8)$$

In the polar coordinates  $(q_\perp, \theta)$  we have  $dq_x dq_y = q_\perp dq_\perp d\theta$  and Eq. (5) becomes

$$W_{r_0} = \frac{2\pi}{\hbar} \delta(E_A - E_0) \left( \frac{e^2}{2(2\pi)^2 \kappa} \right)^2 \times \left| \int_{q_\perp, \theta} \frac{q_\perp dq_\perp d\theta}{(q_\perp + q_s)(1 + q_\perp/b)^3} f_{A,L}^{2D}(\mathbf{q}) \right|^2. \quad (9)$$

To obtain the full rate of transitions between a free state and an acceptor state, one should sum over the density of final states. This gives

$$W_{L,A} = \int_{r_0} W_{r_0} N_A dx_0 dy_0 = \int_E W_{r_0} N_A \frac{dE}{eF} dx_0. \quad (10)$$

To make the calculation tractable, we approximate  $W_{r_0}$  by its value for  $x_0 = 0$ , and sum over an interval  $2l_B$  in which the overlap between the initial and final wave functions is finite. We finally obtain the following transition rate for one electron:

$$W_{L,A}^{\text{imp}} = \frac{l_B N_A e^4}{2(2\pi)^2 8\pi^2 \hbar e F \kappa^2} \times \left| \int_{q_\perp, \theta} \frac{q_\perp dq_\perp d\theta}{(q_\perp + q_s)(1 + q_\perp/b)^3} f_{A,L}^{2D}(\mathbf{q}) \right|^2. \quad (11)$$

The reciprocal process, characterized by the transition rate for one electron  $W_{A,L}^{\text{imp}}$ , is described by the above formula with  $N_A$  replaced by the density of Landau states  $eB/h$ . In our case ( $\nu = 1$ ) there is  $eB/h = N_s$ . For sample 35A55 we have  $N_s = 1.36 \times 10^{11} \text{ cm}^{-2}$  and  $N_A = 0.4 \times 10^{11} \text{ cm}^{-2}$ . Therefore, considering one electron, transitions to free states are more probable than transitions to acceptor states. This is seen in Fig. 12, where  $W_{A,L}^{\text{imp}} > W_{L,A}^{\text{imp}}$ . We remark that Eq. (11) gives

$$N_s \times W_{L,A}^{\text{imp}} = N_A \times W_{A,L}^{\text{imp}}. \quad (12)$$

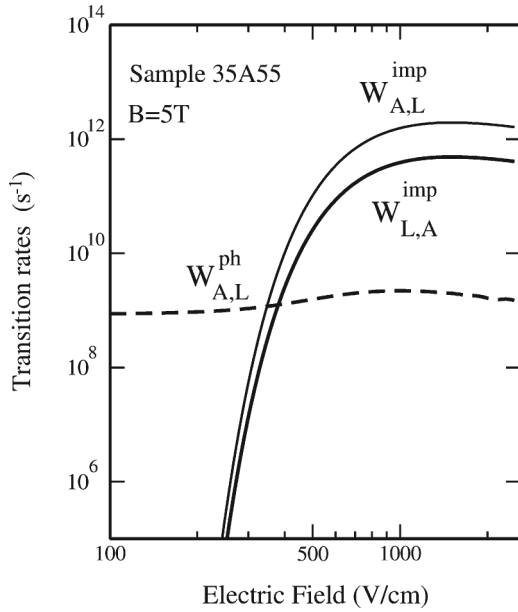


FIG. 12. Calculated electron transition rates of impurity-induced (imp) and phonon-induced (ph) transitions versus electric field. Calculations are carried for  $B = 5$  T.

Figure 12 shows the numerically calculated transition rates as functions of the electric field. There is a steep increase of transition rates when the electric field exceeds 200 V/cm. This occurs as a result of overlap of the Landau and acceptor wave functions. Because of the Gaussian shape of both functions the overlap increases exponentially as the orbit centers come close at higher electric fields. The impurity-induced transitions between  $|\psi_L\rangle$  and  $|\psi_A\rangle$  states in the presence of an electric field occur in both directions. In order to fill the acceptor states, the impurity scattering must dominate over the phonon-induced relaxation. The latter enables efficient electron recombination from the acceptor states to the free states at lower energies, as shown in Fig. 13. Let us consider the acoustical phonon scattering and calculate the corresponding transition rate for one electron. As seen in Fig. 13, the energy conservation must fulfill the dispersion relation for acoustic phonons, that is,  $E_A - E_0 = \hbar c_s q_0$ . Because of the electric potential drop, there is  $E_A - E_0 = eFy_0 + \varepsilon_0$ , which gives  $\hbar c_s q_0 = eFy_0 + \varepsilon_0$ . This determines the phonon wave vector  $q_0$  as a function of

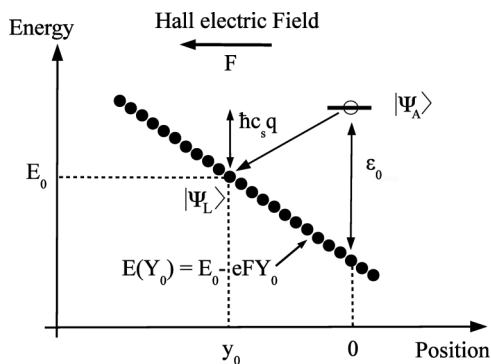


FIG. 13. A localized electron scattered by a phonon to a free state. The energy change fulfills phonon dispersion relation  $\varepsilon(q_0) = \hbar c_s q_0 = \varepsilon_0 + eFy_0$ .

$y_0$ . This equality is imposed in the Fermi golden rule by the Dirac  $\delta$  function. The transition probability due to phonons is<sup>16</sup>

$$W_{r_0} = \frac{2\pi}{\hbar} \int_{\mathbf{q}} \frac{\Omega d^3\mathbf{q}}{(2\pi)^3} \frac{\hbar(n_q + 1)q^2 \mathcal{E}_1^2}{2\mu_v \Omega c_s q} \times |f_{A,L}(\mathbf{q})|^2 \delta(E_A - E_0 - \hbar c_s q), \quad (13)$$

where  $\mathcal{E}_1$  is the deformation potential of the electron-phonon interaction,  $\Omega$  is the crystal volume,  $\mu_v$  is the crystal density,  $c_s$  is the sound velocity, and

$$f_{A,L}(\mathbf{q}) = f_{A,L}^{2D}(\mathbf{q}_{\perp}) \int_z f_0^2(z) e^{iq_z z} dz = \frac{f_{A,L}^{2D}(\mathbf{q}_{\perp})}{(1 + q_z^2/b^2)^{3/2}} \quad (14)$$

is the form factor of the complete 3D wave function, with  $b$  calculated from the heterostructure characteristics.<sup>17</sup> For sample 35A55 we calculate  $b = 3 \times 10^8 \text{ m}^{-1}$ .

Introducing cylindrical coordinates  $(q_{\perp}, \theta, q_z)$  we have  $dq_x dq_y dq_z = q_{\perp} dq_{\perp} d\theta dq_z$ . Then Eq. (13) gives

$$W_{x_0, y_0} = \frac{\mathcal{E}_1^2}{8\pi^2 \mu_v \hbar c_s^2} \int_{q_z=0}^{q_0} \frac{dq_z}{(1 + q_z^2/b^2)^3} \times \int_{q_{\perp}, \theta} q_{\perp} dq_{\perp} d\theta (n_q + 1) \delta(q_0 - q) \times \left| \int_{x,y} \psi_L(\mathbf{r} - \mathbf{r}_0) \psi_A(\mathbf{r}) e^{iq_{\perp} \cdot \mathbf{r}} dx dy \right|^2, \quad (15)$$

where the value  $q_0$  is given by the relation  $\hbar c_s q_0 = eFy_0 + \varepsilon_0$ . When  $q_z$  is fixed,  $q^2 = q_{\perp}^2 + q_z^2$  and  $q_{\perp} dq_{\perp} = q dq$ . We replace the integration over  $q_{\perp}$  by an integration over  $q$  which is straightforward. In addition, we approximate  $(n_q + 1) \approx 1$  because at 4.2 K there are very few phonons. This gives

$$W_{x_0, y_0} = \frac{\mathcal{E}_1^2}{8\pi^2 \mu_v \hbar c_s^2} \int_{q_z=0}^{q_0} \frac{dq_z}{(1 + q_z^2/b^2)^3} \int_{\theta} d\theta q_0^2 \times \left| \int_{x,y} \psi_A(\mathbf{r}) \psi_L(\mathbf{r} - \mathbf{r}_0) e^{iq_{\perp} x \cos \theta} e^{iq_{\perp} y \sin \theta} dx dy \right|^2, \quad (16)$$

where  $q_{\perp} = \sqrt{q_0^2 - q_z^2}$  in the last integral. The total transition rate is obtained by summing over all final free states  $\mathbf{r}_0$ . To make the calculation tractable we restrict again the integration over  $y_0$  to an interval of the width  $2l_B$  in which the overlap of the wave functions is significant. Also, we take in  $W_{r_0}$  approximately  $x_0 = 0$ . This gives

$$W_{A,L} = 2l_B N_s \int_{y_0=-\infty}^{+\infty} W_{0, y_0} dy_0, \quad (17)$$

and we finally obtain for one electron

$$W_{A,L}^{\text{ph}} = \frac{l_B N_s \mathcal{E}_1^2}{4\pi^2 \mu_v \hbar c_s^2} \int_{y_0} dy_0 \int_{q_z, \theta} \frac{dq_z d\theta}{(1 + q_z^2/b^2)^3} q_0^2 \times \left| \int_{x,y} \psi_L(\mathbf{r} - \mathbf{r}_0) \psi_A(\mathbf{r}) e^{iq_{\perp}(x \cos \theta + y \sin \theta)} dx dy \right|^2. \quad (18)$$

The values of  $W_{A,L}^{\text{ph}}$  were calculated numerically and the results are shown in Fig. 12. It can be seen that the electric field has little influence on the phonon transition rate. The latter remains almost constant at the considered electric field interval because the recombination to a lower energy state exists even at vanishing electric field.

Now we calculate the occupation of the electron states by counting the incoming and the outgoing electrons. We define the occupancy  $f_L$  as a ratio of the number of occupied free states to the total number of these states. Similarly, the occupancy  $f_A$  is the ratio of the number of occupied acceptor states to the total number of these states. To obtain the steady state solution for the occupancy functions we make equal the number of electrons per unit time going into acceptor states (term on the left in equation below) and the number of electrons per unit time going out of these states (term on the right). This results in the master equation

$$W_{L,A}^{\text{imp}} N_s f_L (1 - f_A) = (W_{A,L}^{\text{ph}} + W_{A,L}^{\text{imp}}) N_A f_A (1 - f_L). \quad (19)$$

At a vanishing electric field, the phonon scattering rate remains nearly constant, while impurity scattering rate is vanishingly low. Thus,  $W^{\text{imp}} \ll W^{\text{ph}}$ . In this limit the master equation gives  $f_A = 0$ , which signifies that at low electric fields the acceptor states remain empty. In contrast, at high enough electric fields, when  $W^{\text{imp}} \gg W^{\text{ph}}$ , phonons do not provide a sufficiently effective recombination process and the impurity scattering redistributes electrons between free and acceptor states. In this limit the master equation is

$$W_{L,A}^{\text{imp}} N_s f_L (1 - f_A) = W_{A,L}^{\text{imp}} N_A f_A (1 - f_L). \quad (20)$$

Applying Eq. (12), we have  $f_L(1 - f_A) = f_A(1 - f_L)$ , whose solution is  $f_A = f_L$ , that is, it gives equal occupancy for both kinds of states. To calculate this occupancy we use conservation of the electron number

$$N_A f_A + N_s f_L = N_s. \quad (21)$$

As a consequence, we obtain for sample 35A55 ( $N_s = 1.36 \times 10^{11} \text{ cm}^{-2}$  and  $N_A = 0.4 \times 10^{11} \text{ cm}^{-2}$ )

$$f = f_A = f_L = \frac{N_s}{N_s + N_A} = 3/4. \quad (22)$$

The above result shows that 1/4 of the free electrons are trapped on the acceptor states, and, as acceptor states are less numerous, 3/4 of them are populated. Thus, the electric field makes the conducting electron density smaller. This leads to what we called the ‘‘boil-off effect.’’ The corresponding experimental situation is shown in Figs. 8 and 10. For intermediate electric fields the general solution is obtained

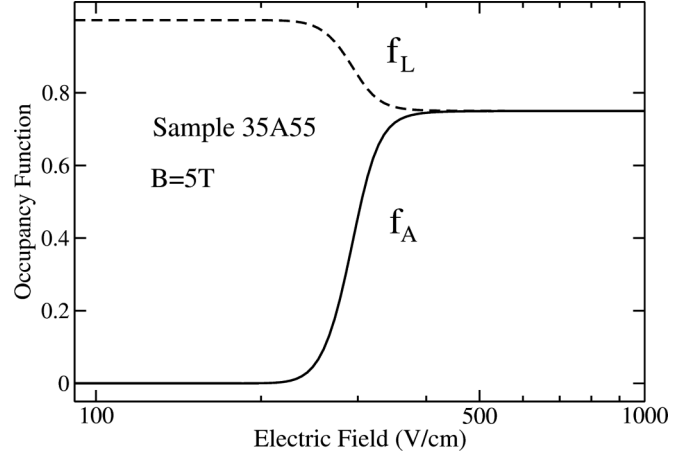


FIG. 14. Calculated occupancy functions for free and acceptor electrons versus electric field for sample 35A55. Above the critical field of 200 V/cm acceptor states become populated and occupancy of the free states diminishes.

by solving the set of equations

$$W_{L,A}^{\text{imp}} N_s f_L (1 - f_A) = (W_{A,L}^{\text{ph}} + W_{A,L}^{\text{imp}}) N_A f_A (1 - f_L), \quad (23)$$

$$N_A f_A + N_s f_L = N_s. \quad (24)$$

The transition rates depend on the electric field and so do the solutions  $f_A$  and  $f_L$ . One finds

$$f_A = \frac{-(\eta + 1) + \sqrt{(\eta + 1)^2 + 4\lambda\eta}}{2\lambda\eta} \quad (25)$$

and

$$f_L = 1 - \eta f_A, \quad (26)$$

where we define  $\lambda = W_{A,L}^{\text{ph}} / W_{A,L}^{\text{imp}}$  and  $\eta = N_A / N_s$ . Solutions are shown as functions of the electric field in Fig. 14. It is seen that, above the critical field, the electrons are trapped in the acceptor states. The critical field above which the localization begins is about 200 V/cm.

## V. DISCUSSION

Previous theoretical analysis showed that in the QHE conditions one can deal with discrete acceptor levels above conduction Landau levels.<sup>6</sup> As a result, in the ultraquantum limit of magnetic fields and low temperatures the electrons fall down from localized acceptor states to free Landau states and begin to conduct. This process, which we call the thaw down effect, is quite natural and we confirm it experimentally. In addition, there exists a possibility to observe an effect inverse to the magnetic freeze-out, in which the electrons go from the free Landau states to the localized acceptor states at higher energies. As a result, these electrons cease to conduct. We call this process the boil-off effect, as proposed originally in Ref. 6. In our experiments the effect is induced by the Hall electric field. The main problem with this interpretation is that the average experimental electric field necessary to the boil-off of electrons in our GaAs/GaAlas samples is around 2 V/cm, whereas the field predicted by the theory is around 200 V/cm, see Fig. 14. However, in studying the breakdown



of QHE many authors observed a large discrepancy between the value of the local electric field and its mean value. The reason for this discrepancy is an important inhomogeneity of the in-plane electric field in the QHE regime.<sup>16,18</sup> Concerning the QHE breakdown, this inhomogeneity was observed and studied by many authors. Chaubet *et al.*<sup>16</sup> demonstrated, using a theoretical and experimental study of transport effects and Landau emission, that the important physical parameter in QHE regime is the *local* electric field and not the mean electric field. It is well known that the in-plane electric field is quite large in the vicinity of current contacts. Klass *et al.*<sup>19</sup> and Komiyama *et al.*<sup>20</sup> performed experiments on Far Infra Red (FIR) emission due to high local electric fields near the contacts. Also Ikushima *et al.*<sup>21</sup> observed in the QHE regime the FIR emission on the edges of the sample, where the local electric field is much higher than in the inner part. In our case of modulation doped quantum wells with a large density of acceptor atoms in the GaAs channel, the electric field inhomogeneity can be larger than in additionally undoped samples. We believe that the discrepancy between the predicted theoretical value and the average experimental value of the critical electric fields which create the boil-off of 2D electrons is only apparent.

As we showed above, the present theory predicts that 1/4 of free electrons can pass to localized magnetoacceptor states and cease to conduct. The experimental increase of resistance shown in Fig. 8 seems to suggest that in reality the transfer of conducting electrons is considerably larger. This result could be reproduced theoretically if a magnetoacceptor could trap more than one conduction electron. We will investigate this possibility in a future work.

## VI. SUMMARY

The purpose of our work was to detect localized magnetoacceptor states in the 2D conduction band by means of the quantum transport. The MA states had been seen in cyclotron resonance experiments but the transport evidence of their existence was missing. With this aim in mind we investigated the quantum Hall effect and the Shubnikov–de Haas effect in *n*-type modulation doped GaAs/GaAlAs quantum wells additionally doped with Be atoms in the conducting channel. The Be atoms are known to create acceptor states in GaAs. Such 2D acceptors localize conduction electrons by a combined effect of the well and a magnetic field. The localized electron states due to acceptors have discrete energies in the conduction

band above the corresponding Landau levels. We observed two effects in the high quantum limit of magnetotransport which we attributed to the localized MA states. The first, which we called the magnetic thaw down effect, is caused by electrons falling down from the MA states to the Landau states when, at a high magnetic field, the Fermi energy is below the MA levels but above the Landau levels. This is manifested experimentally by a shift of the Hall plateau toward higher magnetic fields. The situation can be regarded as an inverted process to that of electron freeze-out from the Landau levels to magnetodonor levels which leads to an increase of resistance due to a decrease of the electron density. The second effect, which we called the magnetic boil-off, is caused by the Hall electric field pushing electrons from the filled Landau levels to the empty MA levels. This process has an avalanche character in our experimental conditions of the constant current, leading to a dramatic increase of magnetoresistance in the ultraquantum limit of magnetic fields. Our work provides an experimental evidence for both effects and our theoretical analysis shows that it is possible to redistribute electrons between free and localized states in the conduction band by an electric field transverse to magnetic field.

## ACKNOWLEDGMENT

We thank Dr. T. M. Rusin for elucidating discussions.

## APPENDIX

We consider here the gauge aspects of our calculations which are not trivial. Equations (2) and (4) give the wave functions in the symmetric gauge  $\mathbf{A}' = [-\frac{1}{2}B(y - y_0), \frac{1}{2}B(x - x_0), 0]$ . On the other hand, the energies of Eq. (1) are given in the asymmetric gauge  $\mathbf{A} = [-By, 0, 0]$ . To use the same gauge throughout we transform the wave function  $\psi'_A$  and  $\psi'_L$  to the asymmetric gauge by performing the transformation<sup>22,23</sup>

$$\mathbf{A} = \mathbf{A}' + \nabla\chi, \quad (\text{A1})$$

$$\psi = \psi' \exp\left(-\frac{ie}{\hbar}\chi\right). \quad (\text{A2})$$

We have  $\chi_A = -\frac{1}{2}By(x - x_0) - \frac{1}{2}Bx_0y_0$  for the acceptor state centered at  $\mathbf{r}_0 = (x_0, y_0)$ , and  $\chi_L = -\frac{1}{2}Byx$  for the Landau state at  $\mathbf{r}_0 = 0$ . We found that calculations performed with  $\psi_A$  and  $\psi_L$  functions do not differ much from those performed with the nontransformed functions  $\psi'_A$  and  $\psi'_L$ .

\*Corresponding author: christophe.chaubet@univ-montp2.fr

<sup>1</sup>T. Ando, A. B. Fowler, and F. Stern, *Rev. Mod. Phys.* **54**, 437 (1982).

<sup>2</sup>E. Brezin, D. J. Gross, and C. Itzykson, *Nucl. Phys. B* **235**, 24 (1984).

<sup>3</sup>S. Bonifacie, C. Chaubet, B. Jouault, and A. Raymond, *Phys. Rev. B* **74**, 245303 (2006).

<sup>4</sup>K. von Klitzing, G. Dorda, and M. Pepper, *Phys. Rev. Lett.* **45**, 494 (1980).

<sup>5</sup>R. B. Laughlin, *Phys. Rev. B* **23**, 5632 (1981).

<sup>6</sup>M. Kubisa and W. Zawadzki, in *Proceedings of the 20th International Conference on Physics in Semiconductors*, edited by E. M. Anastassakis and J. D. Joannopoulos (World Scientific, Singapore, 1990), p. 159; *Semicond. Sci. Technol.* **11**, 1263 (1996).

<sup>7</sup>P. Vincente, A. Raymond, M. Kamal-Saadi, B. Couzinet, M. Kubisa, W. Zawadzki, and B. Etienne, *Solid State Commun.* **96**, 901 (1995).

<sup>8</sup>S. Bonifacie, Y. M. Meziani, S. Juillaguet, C. Chaubet, A. Raymond, W. Zawadzki, V. Thierry-Mieg, and J. Zeman, *Phys. Rev. B* **68**, 165330 (2003).

- <sup>9</sup>A. M. Chang, in *The Quantum Hall Effect*, edited by R. E. Prange and S. M. Girvin (Springer, New York, 1987), p. 175.
- <sup>10</sup>R. J. Haug, R. R. Gerhardt, K. von Klitzing, and K. Ploog, *Phys. Rev. Lett.* **59**, 1349 (1987).
- <sup>11</sup>J. E. Furneaux and T. L. Reinecke, *Phys. Rev. B* **33**, 6897 (1986).
- <sup>12</sup>A. Raymond, I. Bisotto, Y. M. Meziani, S. Bonifacie, C. Chaubet, A. Cavanna, and J. C. Harmand, *Phys. Rev. B* **80**, 195316 (2009).
- <sup>13</sup>J. L. Robert, A. Raymond, L. Konczewicz, C. Bousquet, W. Zawadzki, F. Alexandre, I. M. Masson, J. P. Andre, and P. M. Frijlink, *Phys. Rev. B* **33**, 5935 (1986); W. Zawadzki, M. Kubisa, A. Raymond, J. L. Robert, and J. P. Andre, *Phys. Rev. B* **36**, 9297 (1987).
- <sup>14</sup>G. Ebert, K. von Klitzing, K. Ploog, and G. Weiman, *J. Phys. C* **16**, 5441 (1983).
- <sup>15</sup>M. E. Cage, R. F. Dziuba, B. F. Field, E. R. Williams, S. M. Girvin, A. C. Gossard, D. C. Tsui, and R. J. Wagner, *Phys. Rev. Lett.* **51**, 1374 (1983).
- <sup>16</sup>C. Chaubet, A. Raymond, and D. Dur, *Phys. Rev. B* **52**, 11178 (1995).
- <sup>17</sup>F. F. Fang and W. E. Howard, *Phys. Rev. Lett.* **16**, 797 (1966).
- <sup>18</sup>P. F. Fontein, P. Hendricks, F. A. P. Blom, J. H. Wolter, L. J. Gilling, and C. W. J. Beenakker, *Surf. Sci.* **263**, 91 (1991).
- <sup>19</sup>U. Klass, W. Dietsche, K. von Klitzing, and K. Ploog, *Z. Phys. B* **82**, 351 (1991).
- <sup>20</sup>S. Komiyama, H. Sakuma, K. Ikushima, and K. Hirakawa, *Phys. Rev. B* **73**, 045333 (2006).
- <sup>21</sup>K. Ikushima, H. Sakuma, S. Komiyama, and K. Hirakawa, *Phys. Rev. Lett.* **93**, 146804 (2004).
- <sup>22</sup>L. D. Landau and E. M. Lifshits, *Quantum Mechanics*, 3rd ed. (Pergamon, Oxford, 1977).
- <sup>23</sup>T. Haugset, Y. Aa. Ruud, and F. Ravndal, *Phys. Scr.* **47**, 715 (1993).